iScience, Volume *26*

Supplemental information

Preclinical safety and efficacy of a therapeutic antibody that targets SARS-CoV-2 at the sotrovimab face but is escaped by Omicron

Jakob Kreye, S. Momsen Reincke, Stefan Edelburg, Lara M. Jeworowski, Hans-Christian Kornau, Jakob Trimpert, Peter Hombach, Sophia Halbe, Volker Nölle, Martin Meyer, Stefanie Kattenbach, Elisa Sánchez-Sendin, Marie L. Schmidt, Tatjana Schwarz, Ruben Rose, Andi Krumbholz, Sophie Merz, Julia M. Adler, Kathrin Eschke, Azza Abdelgawad, Dietmar Schmitz, Leif E. Sander, Uwe Janssen, Victor M. Corman, and Harald Prüss

SUPPLEMENTAL INFORMATION

Preclinical safety and efficacy of a therapeutic antibody that targets SARS-CoV-2 at the Sotrovimab face but is escaped by Omicron

Jakob Kreye, S Momsen Reincke, Stefan Edelburg, Lara M Jeworowski, Hans-Christian Kornau, Jakob Trimpert, Peter Hombach, Sophia Halbe, Volker Nölle, Martin Meyer, Stefanie Kattenbach, Elisa Sánchez-Sendin, Marie L Schmidt, Tatjana Schwarz, Ruben Rose, Andi Krumbholz, Sophie Merz, Julia M. Adler, Kathrin Eschke, Azza Abdelgawad, Dietmar Schmitz, Leif E Sander, Uwe Janssen, Victor M Corman, Harald Prüss

Table S1. Functional properties, analytical measurements and *in silico* predictions of HEK cell produced therapeutic mAb candidates, Related to Figures 1 and 2

mAb	**SARS-CoV-2 RBD affinity** (K_D in M, from SPR)	**SARS-CoV-2 neutralization** (IC_{50} in ng/ml, from PRNT)	**SARS-CoV binding** (from ELISA)	**Murine tissue reactivity** (from immunohistology)	**Formulation and application** (pI value, from IEF)	**Aggregation behaviour** (Monomer content in %, from SEC)	**Structural stability** (Inflection temperature in °C, from NanoDSF)	**|----------Bioinformatic sequence predictions----------|**										
										Therapeutic Antibody Profiler (TAP)					**AGGRE SCAN**		**Protein-Sol**	
								Tm #1	Tm #2	Critical CDR motifs	CDRsL	PSH	PPC	PNC	SFv CSP	Na4vSS VHC	Na4vSS VLC	PSSV VHC	PSSV VLC
CV05-163	2.2E-10	16.3	No	No	≥ 8.7	100	73.8	89.2	Yes	52	149.3	0	0.08	12	-1.3	-3.6	0.56	0.44
CV07-200	n/a	14.5	No	Yes	n/a	n/a	n/a	n/a	n/a	n/a	n/a	n/a	n/a	n/a	n/a	n/a	n/a	n/a
CV07-209	6.0E-12	3.1	No	No	7.7 - 8.2	99.7	73.6	84.1	No	46	118.2	0	0.25	-6	7.4	-6.6	0.47	0.67
CV07-222	6.97E-12	7.8	No	Yes	8.6 (calc.)[1]	n/a	n/a	n/a	No	57	149.2	1.16	0.04	6.4	1.1	-5.0	0.50	0.60
CV07-250	5.64E-11	3.5	No	No	5.8 - 6.6	67.8	61.8	71.1	Yes[2]	53	144.6	2.47	0.26	-7.2	-5.3	-8.8	0.68	0.65
CV07-255	n/a	14.5	No	Yes	8.3 (calc.)[1]	n/a	n/a	n/a	Yes	53	131.1	1.20	0.18	-3.2	-0.9	-6.4	0.45	0.57
CV07-262	7.9E-11	7.1	No	No	≥ 8.7	98.2	73.7	87.6	Yes	60	153.9	1.16	0.04	6.2	1.6	-4.1	0.57	0.57
CV07-270	n/a	82.3	No	Yes	8.6 (calc.)[1]	n/a	n/a	n/a	No	60	146.6	0.35	0	0.5	3.4	-4.1	0.58	0.61
CV07-283	4.75E-11	16.9	No	No	≥ 8.7	100	74.5	83.7	No	56	145.6	0	0	4.2	-0.4	-5.1	0.50	0.63
CV07-287	1.6E-10	41.7	No	No	8.4 (calc.)[1]	n/a	n/a	n/a	Yes[3]	51	120.4	0	0.05	6	1.1	-3.9	0.48	0.46
CV07-315	1.12E-11	24.9	No	No	≥ 8.7	99.8	73.1	87.1	Yes	55	162.3	1.14	1.12	-1.6	-1.6	-7.4	0.36	0.62
CV38-113	1.34E-10	20.8	No	No	7.8 - 8.3	98.5	75.1	88.5	No	47	176.1	0.08	0.41	-6.2	1.5	-8.0	0.49	0.67
CV38-139	2.77E-10	73.2	No	No	≥ 8.7	91.6	75.7	89.3	Yes	44	124.9	0	0	3.3	4.5	1.0	0.49	0.56
CV38-142	1.05E-09	23.2	Yes	No	≥ 8.7	96	74.8	89.1	No	52	132.0	0.20	0.20	4.4	6.5	-4.3	0.57	0.67
CV38-183	5.93E-11	3.7	No	No	7.8 - 8.3	98.3	73.2	88	Yes	53	160.0	0	0.22	1.1	1.1	-6.9	0.50	0.56
CV38-221	4.99E-10	172.6	No	No	8.2 (calc.)[1]	n/a	n/a	n/a	No	41	127.7	0	0	4	7.6	-2.1	0.50	0.42
CV-X1-126	2.43E-10	71.7	No	No	≥ 8.7	100	75.2	87.6	Yes	44	125.7	0	0.11	9.3	0.5	-0.6	0.50	0.56
CV-X2-106	n/a	17.6	No	No	8.4 (calc.)[1]	n/a	n/a	n/a	No	52	175.3	1.14	0.08	6	3.2	0.4	0.60	0.58

[1] only calculated pI values are available

[2] N-glycosylation site in HCDR1

[3] cysteine in HCDR3

For the 18 indicated mAbs that had previously been identified by their high potency for SARS-CoV-2 neutralization (Kreye et al., 2020) functional properties, analytical measurements and *in silico* predictions, all from HEK cell produced material, are shown to evaluate their potential for the development into a therapeutic antibody. The functional properties of SARS-CoV-2 RBD affinity

(measured by surface plasmon resonance (SPR)), SARS-CoV-2 neutralization (by authentic virus plaque reduction neutralization tests (PRNT)), SARS-CoV binding (by RBD ELISA) and murine tissue reactivity (by immunohistochemistry on unfixed tissue sections) have previously been investigated ((Kreye et al., 2020), Table S3). The evaluation of the biophysical properties by analytical measurements include the evaluation of formulation and application (by isoelectric point (pI) measurements using isoelectric focusing (IEF)), aggregation behavior (by monomer content quantification using size exclusion chromatography (SEC)) and structural stability (by inflection temperature measurements using nano differential scanning fluorimetry (NanoDSF)). Furthermore, antibody sequences were analyzed for critical CDR sequence motifs and by *in silico* predictions using Therapeutic Antibody Profiler (TAP), AGGRESCAN and Protein-Sol to evaluate the total length of CDRs (CDRsL), the extent of hydrophobicity as measured by patches of surface hydrophobicity (PSH), the regions of dense charge as measured by number of patches of positive and of negative charge (PPC, PNC), the asymmetry in the net heavy and light chain surface charge as measured by the structural Fv charge symmetry parameter (SFvCSP), the normalized a4v sequence sum for 100 residues (Na4vSS) and the predicted scaled solubility value (PSSV) for the variable heavy and light chains (VHC, VLC). Criteria for classification as favorable, neutral or unfavorable for all parameters are described with the methods section and classification displayed in Figure 1A. n/a = not available.

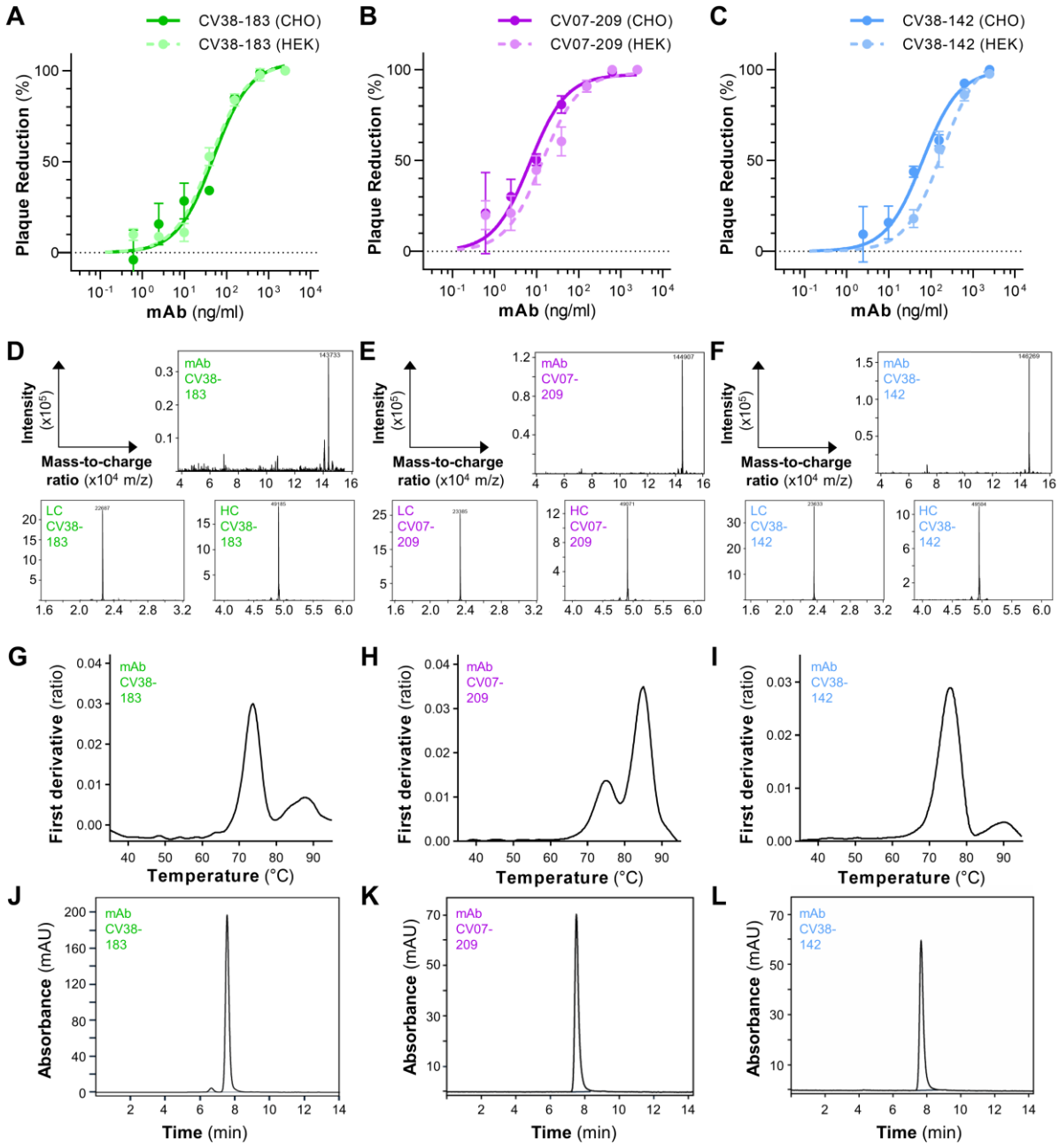

M

mAb	IC_{50} (ng/ml)	Measured / calculated mass (m/z)				Inflection temperature (°C)		Monomer content (%)
		LC		HC				
		calculated	measured	calculated	measured	Tm #1	Tm #2	
CV38-183	49.1	22686	22687	49184	49185	73.7	87.7	97
CV07-209	6.9	23384	23385	49071	49071	75.3	84.9	100
CV38-142	63.7	23632	23633	49503	49504	75.6	90.0	100

Figure S1. Comparability and quality control of CHO cell produced mAbs, Related to Figure 2

(A-C) Concentration-dependent neutralization of plaque formation from authentic wildtype SARS-CoV-2 isolate by indicated mAbs. Purified mAbs from CHO cell line production or from transient HEK cell

production were used as indicated. Non-linear regression models are shown. Values indicate mean ± SD from two independent measurements.

(D-F) Mass spectrometry measurements are shown for full mAbs (top) and light chain (LC, bottom left) and heavy chain (HC, bottom right) after reduction of the indicated mAbs from CHO cell line production after removal of N-linked glycans by PNGase F treatment to confirm intact mass.

(G-I) Temperature-dependent emission wavelength measurements of tryptophan fluorescence at 350 and 330 nm (first derivative of the ratio) using nano differential scanning fluorimetry are shown for the indicated mAbs produced in CHO cell line. The derived inflection temperature is used to evaluate the mAb's structural stability.

(J-L) Size exclusion chromatography is shown for the indicated mAbs from CHO cell line production as quality control measure to evaluate the level of aggregation. A retention time of ~ 7.8 min corresponds to an apparent molecular weight of ~ 160 kDa.

(M) Data table displaying results of measurements shown in (A-L) with indicated mAbs from CHO cell line production.

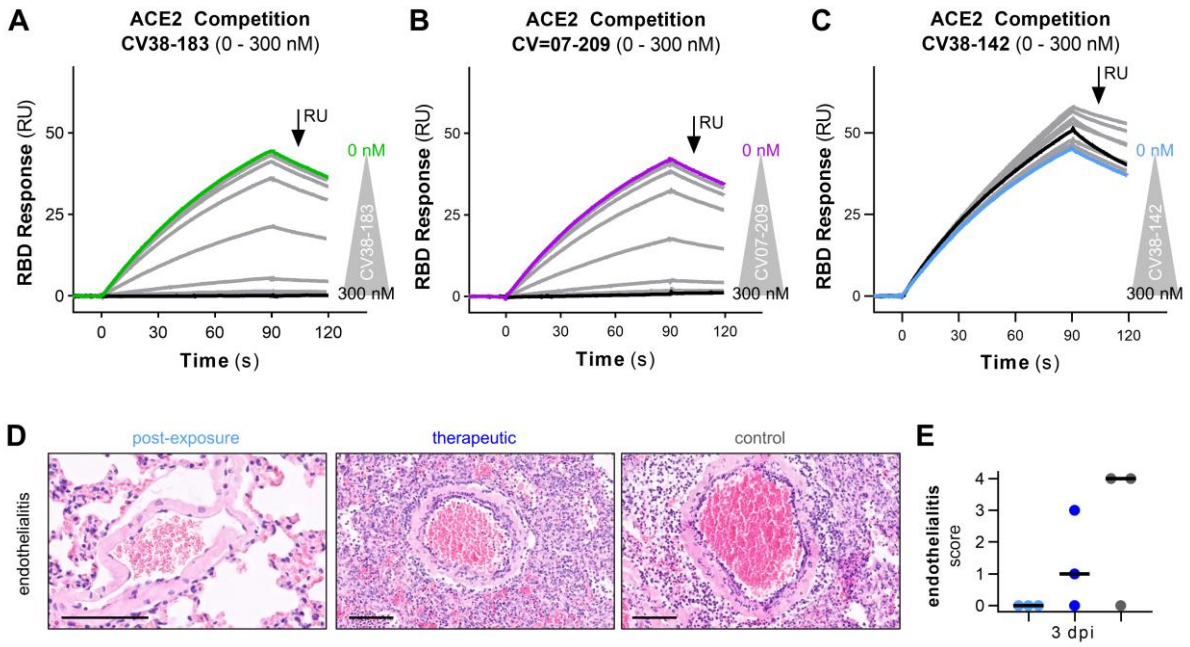

Figure S2. ACE2 competition analysis using SPR measurements and endothelialitis scoring in hamster lungs, Related to Figures 2 and 3 and Table S2

(A-C) Exemplary quantifications of RBD binding to an immobilized Avi-tagged ACE2 protein using SPR. The traces represent independent measurements at varied concentrations of the indicated mAbs. The responses at the indicated time point as mean from two independent measurements were used to determine non-linear regression models and derived mAb concentrations of half-maximal competition of the RBD-ACE2 interaction (IC_{50}) (shown in Figure 2D) to evaluate the competition of RBD-ACE2 interaction by the mAbs. The colored traces depict the recordings from non-competition condition with mAb at 0 nM, black traces indicate recordings with mAb at highest concentration (300 nM).

(D) Histopathology of representative hematoxylin and eosin stained, paraffin-embedded lung tissues at 3 dpi. Lung parenchyma magnifications with pulmonary blood vessels revealed marked endothelialitis as a characteristic sign of SARS-CoV-2 lung pathology in control animals (right). In animals of the therapeutic group (center) endothelialitis was present but less animals were affected, whereas in animals of the post-exposure group (left) no endothelialitis or vascular lesions were apparent. Scale bars: 100 µm.

(E) Corresponding histopathological endothelialitis scores at 3 dpi are shown. Bars indicate median.

Table S2. Histopathological scoring of hamster lung tissue from SARS-CoV-2 VOC infection model, Related to Figures 3 and S2

animal number	time point (dpi)	% of pneumonia affected lung tissue	Severity of pneumonia [a,*]	Infiltration of lymphocytes [b]	Infiltration of makrophages [b]	Infiltration of neutrophils [b]	Infiltration of heterophils	Broncial epithelial cell (BEC) necrosis [a]	BEC hyperplasia	Bronchitis [a]	Bronchiolitis	Hyaline membranes	Alveolar epithelial cell (AEC) necrosis	AEC Type II hyperplasia [a]	Alveolar edema [c]	Perivascular edema [c]	Perivascularlymphocytic cuffing (PLC) [b]	Bronchus-associated lymphoid tissue (BALT)	Endothelialitis	Hyaline thrombi	Alveolar hemorrhage	[a] Lung Inflammation Score	[b] Immune Cell Infiltration Score	[c] Edema Score
P1	3	5-10	1	1	1	2	0	2	0	2.5	1.5	0	0	0	0	0	0	0	0	0	0	1.4	1.0	0.0
P2	3	0	0	0	0	0	0	0	0	1	0	0	0	0	0	0	0	0	0	0	0	0.3	0.0	0.0
P3	3	<5	1	1	1	2	0	0	0	1	1	0	0	0	0	0	0	0	0	0	0	0.5	1.0	0.0
T1	3	20-30	2.5	2	3	3	1	0	0	1	1.5	0	2	0	1.5	0	1	0	1	0	0	0.9	2.3	0.8
T2	3	<5	1	1	1	1	1	0	0	1	1	0	0	0	0	0	0	0	0	0	0	0.5	0.8	0.0
T3	3	40	3.5	2	3	4	1.5	0	0	1	1.5	0	2.5	0	0	0	2	0	3	0	1	1.1	2.8	0.0
C1	3	40-50	3.5	2	3	3.5	1.5	0	2	0	1.5	0	3	0	3	2.5	3	0	4	0	0	0.9	2.9	2.8
C2	3	5	1	1	1	2	0	0	0	2.5	0	0	0	0	0	0	0	0	0	0	0	0.9	1.0	0.0
C3	3	70	4	2.5	3	3.5	1	0	2.5	1	1	0	3	0	2	2.5	3	0	4	0	1	1.3	3.0	2.3
P4	5	60	3.5	2	3.5	3.5	1	0	3.5	1	1.5	0	3	4	1	3.5	2.5	0	3.5	0	1	2.1	2.9	2.3
P5	5	0	0	0	0	0	0	0	0	1	0	0	0	0	0	0	0	0	0	0	0	0.3	0.0	0.0
P6	5	<5	1	1	2	2	1	0	0	1	1	0	1	0	0	0	0	0	0	0	0	0.5	1.3	0.0
T4	5	<5	1	1	1	2	2	0	0	1	0	0	0	0	0	0	0	0	0	0	0	0.5	1.0	0.0
T5	5	<5	1	1	1	2	0	0	0	1	1	0	0	0	0	0	0	0	0	0	0	0.5	1.0	0.0
T6	5	0	0	0	0	0	0	0	0	0	0	0	0	0	0	0	0	0	0	0	0	0.0	0.0	0.0
C4	5	60	4	2.5	3.5	3.5	2	0	2.5	1	0	0	3	4	3	3.5	2	0	2	0	4	2.3	2.9	3.3
C5	5	60	3.5	2.5	3.5	4	1.5	0	2	1.5	1.5	0	3	2.5	3	3	2.5	0	3	0	1	1.9	3.1	3.0
C6	5	90	4	2.5	4	4	1	0	1	0	1.5	0	2.5	2	2.5	2.5	2	0	2	0	1	1.5	3.1	2.5
P7	7	0	0	0	0	0	0	0	0	1	0	0	0	0	0	0	0	0	0	0	0	0.3	0.0	0.0
P8	7	0	0	0	0	0	0	0	0	1	0	0	0	0	0	0	1	0	0	0	0	0.3	0.3	0.0
P9	7	0	0	0	0	0	0	0	0	0	0	0	0	0	0	0	0	0	0	0	0	0.0	0.0	0.0
T7	7	20-30	2.5	2	3	3	1	0	0	0	0	0	1.5	2.5	0	1	0	0	0	0	0	1.3	2.0	0.5
T8	7	40	3.5	2	3	4	2	0	2	0	1	0	2.5	4	1	3	1	0	0	0	2	1.9	2.5	2.0
T9	7	40	3.5	2	3	4	1.5	0	2	0	0	0	3	3.5	0	2	1	0	0	0	0	1.8	2.5	1.0
C7	7	70	4.0	2.5	3.5	3.5	2	0	3	1	2	0	3.5	4	3	3	3	0	4	0	3	2.3	3.1	3.0
C8	7	70	4.0	2.5	3.5	3.5	1.5	0	1	1.5	1	0	3	4	2.5	3.5	3	0	0	0	1	2.4	3.1	3.0
C9	7	80	4.0	2.5	4	4	1	0	1	0	0	0	3.5	4	3	2.5	2.5	0	0	0	0	2.0	3.3	2.8

Histopathological scoring of formalin-fixed paraffin-embedded lung tissue from hamsters of experimental groups as abbreviated (P = post-exposure, T = therapeutic, C = control) at indicated days post infection (dpi). Severity of pneumonia (*) is scaled as (1) minimal, (2) mild, (3) moderate or (4) severe. For all other parameters rating refers to occurrence rate from (1) sporadic, (2) mild, (3) moderate to (4) severe. The scores in the right columns were assessed as means from parameters with corresponding letters as indicated.

Table S3. Analysis of buried surface areas and interactions of RBD-mAb interfaces, Related to Figure 5

CV38-142

RBD Residue (Amino Acid)	BSA HC (Å²)	BSA LC (Å²)	RBD Residue (Atom)	Distance (Å)	mAb Residue (Atom)	Interaction
F342	3.50	0.00				
N343	51.11	0.00	ASN343[OD1]	2.9	HC:SER100[N]	H
A344	1.11	0.00				
T345	99.27	0.00				
R346	66.34	0.00				
S373	25.89	0.00				
W436	28.11	0.00				
N437	13.14	0.00				
S438	3.85	0.00				
N439	0.00	0.98				
N440	34.73	93.72	ASN440[ND2]	3.6	LC:TYR92[O]	H
L441	117.69	0.24	LEU441[O]	2.8	HC:ARG58[NH1]	H
D442	2.63	0.00				
S443	5.94	8.38				
K444	72.68	3.51	LYS444[NZ]	2.9	HC:THR57[O]	H
			LYS444[NZ]	2.9	HC:ASP56[OD1]	H
V445	18.52	45.56				
N448	16.24	0.00				
N450	61.04	0.00	ASN450[ND2]	3.2	HC:SER55[O]	H
			ASN450[ND2]	3.7	HC:ASP56[OD2]	H
P499	0.00	10.20				
R509	7.48	0.00				

Sotrovimab

RBD Residue (Amino Acid)	BSA HC (Å²)	BSA LC (Å²)	RBD Residue (Atom)	Distance (Å)	mAb Residue (Atom)	Interaction
I332	7.29	0.00				
N334	69.01	0.00				
L335	69.92	0.00				
P337	45.14	0.00				
G339	12.18	0.00				
E340	114.19	0.00	GLU340[OE1]	3.0	HC:ALA104[N]	H
			GLU340[OE1]	2.9	HC:TRP105[N]	H
			GLU340[OE2]	3.0	HC:PHE106[N]	H
V341	1.67	0.00				
F342	2.20	0.00				
N343	65.68	0.00	ASN343[ND2]	3.3	HC:TYR100[OH]	H
			ASN343[O]	2.8	HC:ILE111[N]	H
A344	21.18					
T345	51.59	56.11	THR345[N]	3.0	HC:SER109[O]	H
			THR345[OG1]	3.3	HC:SER109[O]	H
			THR345[O]	3.7	LC:THR32[OG1]	H
R346	23.35	53.77	ARG346[NH2]	3.3	HC:SER109[OG]	H
			ARG346[NH1]	3.4	LC:ASP93[O]	H
			ARG346[NH2]	3.7	LC:HIS92[O]	H
			ARG346[NH2]	3.1	LC:ASP93[O]	H
N354	9.19	0.00				
K356	63.35	0.00	LYS356[NZ]	2.8	HC:GLU108[OE2]	H
			LYS356[NZ]	3.8	HC:GLU108[OE1]	S
			LYS356[NZ]	3.8	HC:GLU108[OE2]	S
R357	16.79	0.00				
I358	4.35	0.00				

S359	14.53	0.00				
N360	2.44	0.00				
C361	4.68	0.00				
N440	0.00	12.27				
L441	19.24	30.48				
K444	0.00	0.84				
V445	0.00	1.17				
R509	4.23	1.97				

Buried surface area (BSA) and interactions of the RBD and the indicated mAbs were derived from previously published structural data for CV38-142 (PDB: 7LM8; (Liu et al., 2021)) and Sotrovimab (PDB: 7JX3; (Piccoli et al., 2020)), respectively, and identified using PDBePISA (Krissinel and Henrick, 2007) (https://www.ebi.ac.uk/pdbe/prot_int/pistart.html). All RBD residues are displayed that are involved in mAb bonds or with BSA > 0 Å² for either heavy chain (HC) or light chain (LC) or the respective mAb. H = hydrogen bond, S = salt bridges.